

3-D INTEGRAL EQUATION ANALYSIS OF GUIDED AND LEAKY WAVES ON A THIN-FILM STRUCTURE WITH 2-D MATERIAL GRATINGS

Hung Y. David Yang

Department of Electrical Engineering and Computer Science
University of Illinois at Chicago, IL 60607-7053

Abstract

This paper presents a 3-D integral equation analysis of guided surface waves and leaky waves on a dielectric layer structure with 2-D implanted periodic dielectric blocks. The electric fields within the implanted periodic blocks are unknowns in the moment method. The method involves a full dyadic Green's function. The guided surface waves and leaky waves are identified as eigenvalues of a deterministic equation resulting from a moment method procedure. The analysis may deal with a variety of irregular and anisotropic implants. The analysis may also deal with layered or grounded structures through the modification of the Green's function. The presented approach is also suitable for the analysis of photonic band gap materials.

I. Introduction

Due to the recent advancement of material technology, there are growing research activities in the electromagnetic applications of advanced (artificial) materials. Many technologies will benefit if the electric or optical properties of materials can be properly controlled. Photonic crystals where wave propagation is prohibited within a certain band are examples of such applications [1]. In addition, thin-film structures containing periodic material implants have been of considerable interest in integrated optics [2], frequency selective surfaces [3], and absorbing materials [4]. In the past, there is considerable work on material layered structures with material gratings, mostly for 2-D structures with gratings in one direction. References [5-8] are some of the additional examples. Layer structures with 2-D gratings had also been investigated, but mostly for scattering applications, such as for absorbers [4] and frequency selective surfaces [3]. There is little work on guided waves and leaky waves on layered structures with 2-D planar gratings.

This paper deals with the field theoretical analysis of guided and leaky waves on a dielectric slab with planar periodic material blocks. The geometry is shown in Figure 1. A rigorous 3-D integral equation moment method is developed, where the full dyadic Green's function for the structure is needed. Although the implants shown in Figure 1 are rectangular blocks, the developed analysis is general enough

for most irregular (not curved) implants. For 2-D material gratings, the guided or leaky wave characteristics are different in different directions. Results of mode diagrams in different propagation directions will be presented. Photonic band structures for bounded modes are also discussed.

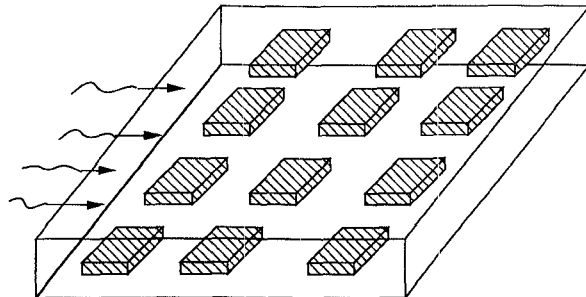


Figure 1. A guided and leaky wave structure with two dimensional material grating within a dielectric slab.

WE
3B

II. 3D Integral Equation Analysis

The geometry is modeled as infinite planar arrays of material blocks within a supporting layer. Since the structure is periodic, Floquet's theorem is applied to simplify the problem to the modeling of electromagnetic waves within an infinitely long cylinder shown in Figure 2. The boundary conditions at the surface of the unit cell are determined on the Floquet's theorem. The cross section of the rectangular cylinder extends within $-a/2 \leq x \leq a/2$ and $-b/2 \leq y \leq b/2$. A material block is at the center of the cell with length L (along the \hat{x} axis), width W (along the \hat{y} axis), and the thickness T (along the \hat{z} axis). The supporting layer with thickness h extends from $-h/2$ to $h/2$. Δ is the distance measured from the bottom of the block to the layer interface (see Figure 2). The region in the cylinder above and below the supporting layer is air regions. ϵ_1 and ϵ_2 are the dielectric constants of the dielectric layer and the implants, respectively. The electric fields within the material block at a unit cell treated as displacement current sources are the unknowns in the moment method analysis. An integral equation is established

to express electric fields in terms of displacement currents. Since all the three components of fields are involved, it is necessary to deal with a full dyadic Green's function for a dielectric slab. The integral equation is expressed as

$$\vec{E} = \iiint_V [G] \cdot \vec{J}_e dv . \quad (1)$$

The volume integral is over only the region of implanted anisotropic material blocks centered at the origin of the Cartesian coordinates. $[G]$ is the dyadic Green's function for a dielectric layer and is in the following form:

$$[G] = \begin{bmatrix} G_{xx} & G_{xy} & G_{xz} \\ G_{yx} & G_{yy} & G_{yz} \\ G_{zx} & G_{zy} & G_{zz} \end{bmatrix} , \quad (2)$$

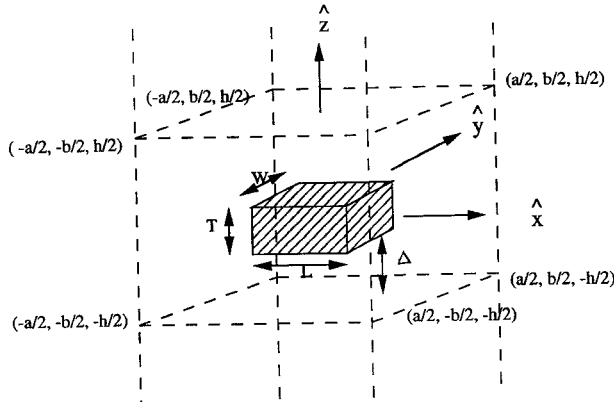


Figure 2. A unit cell of infinite planar arrays of material blocks within a dielectric layer.

with

$$G_{uv} = \frac{1}{ab} \sum_{m=-\infty}^{\infty} \sum_{n=-\infty}^{\infty} \tilde{G}_{uv} e^{-jk_x(x-x')-jk_y(y-y')} , \quad (3)$$

$k_x = \frac{2m\pi}{a} + \beta_x$ and $k_y = \frac{2n\pi}{b} + \beta_y$. u or v is either x , y , or z . β_x and β_y are the propagation constants in the x and y directions, respectively. \tilde{G}_{uv} is the spectral Green's function component and is a function of spectral variables k_x and k_y , z , z' , and the material parameters. The spectral Green's function for a dielectric layer is found in a similar way as that for a microstrip antenna structure. The displacement currents within the implants are in the following form:

$$\vec{J}_e = j\omega\epsilon_0(\epsilon_2 - \epsilon_1)\vec{E} . \quad (4)$$

After the integral equation and the associate Green's function are found, a finite-element moment-method procedure is applied numerically to determine the electric fields within the material implants. This is done first by discretizing the material implants into many small cells within which the fields are assumed (constants), but with unknown coefficients.

$$\vec{E} = \sum_{m_x=1}^{M_x} \sum_{m_y=1}^{M_y} \sum_{m_z=1}^{M_z} \vec{A}_{m_x m_y m_z} f(m_x, m_y, m_z) \quad (5)$$

where within the cell (m_x, m_y, m_z) , $f(m_x, m_y, m_z) = 1$ and $f(m_x, m_y, m_z) = 0$, elsewhere. There are M_x , M_y , and M_z divisions in each side of the material blocks (the x , y , and z directions respectively). If the field representation in Eq. (5) is used in the integral equations and the resulting fields are evaluated at the cell at indices m_x , m_y and m_z , respectively for the x , y , and z directions, we convert the integral equations into a set of linear equations (a matrix equation):

$$\vec{A}_i = \sum_j \sum_{m=-\infty}^{\infty} \sum_{n=-\infty}^{\infty} [g]_{ijmn} \cdot \vec{A}_j (\epsilon_2 - \epsilon_1) , \quad (6)$$

where each i or j represents a particular cell and field component and $[g]_{ijmn}$ is a 3 by 3 matrix resulting from two volume integrations of Eq. (3) over the cells associated with i and j . If both indices i and j run from 1 to $P = 3 \times M_x \times M_y \times M_z$, Eq. (6) represents a matrix equation. Nontrivial solution for the fields requires the matrix determinant to be zero, which results a characteristic equation. The eigenvalues (propagation constants) β are obtained from the roots of this equation through a bisection method.

III. Results and Discussions

One of the features of the moment method is that the shape of the implants is flexible. In the process of solving the matrix equations for rectangular blocks, we may, at our wish, set the displacement currents at some of the cells to zero. This procedure corresponds to physically cutting off pieces of the implants. All the numerical results in this work are produced from PCs. Extended validity check of the present analysis is performed. First, the implanted blocks are set as large as the unit cell, so that the analytic results for the guided wave modes and the plane wave reflection are available. Excellent agreement is found. Another test case is for a plane wave scattering from a slab with one dimensional grating. In this analysis, if the implanted blocks are connected to one of the cell boundary, the geometry reduces from two dimensional to one dimensional gratings. The computed results are compared against those with a finite element method [8]. It is noted

that in this analysis, for higher the frequencies or larger the dimensions, more expansion cells are needed to obtain reasonable convergence. In general, the cell size at about a tenth of wave length provides good convergence. It is also found that the number of cells in the vertical (z) direction is more crucial. In this paper, 441 Floquet modes with $M_x = 3, M_y = 3, M_z = 7$ are used to produce the results.

Guided waves and leaky waves on a dielectric layered structure with 1-D material gratings have been studied extensively and their characteristics are well understood. For 2-D material gratings, it is of interest to investigate the mode characteristics on various directions and the photonic band structures. Examples of dispersion diagrams for guided and leaky wave modes of a dielectric layer with 2-D rectangular material gratings are shown in Figures 3 and 4, respectively for propagation in the \hat{x} and $\hat{x} + \hat{y}$ directions (see Figure 2). For waves in the \hat{x} direction, the mode characteristics are similar to the case for 1-D grating. There exist photonic band gaps for modes near the Brillouin zone boundary. At low frequencies, the two fundamental modes are similar to a TE (upper) and a TM (lower) modes of a dielectric slab. When the frequencies are such that Bragg condition is satisfied, the bounded modes turn to improper complex wave modes (band gap zone). As frequency increases further, bounded surface wave modes (in slow wave zone) turn into proper leaky wave modes (in the fast wave zone). The frequency where the first leaky wave mode turns on and the frequency band where only one leaky wave mode exist are of practical interest. These are determined by the profile of the gratings.

For wave propagation in the $\hat{x} + \hat{y}$ (45^0) direction, the mode diagram is more complicate and is shown in Figure 4. As compared to waves in the \hat{x} direction, the bounded wave modes may exist at higher frequencies and the first leaky wave mode also turns on at a higher frequency. It is very interesting to observe from Figure 4 that the some of the bounded and leaky wave modes are almost degenerate modes.

The photonic band structures for the bounded (slow wave) modes of a dielectric layer with rectangular holes drilled through are shown in Figure 5. In the diagram, between Γ and X points, the modes are propagating in the \hat{x} direction, while between M and Γ points, the modes are propagating in the $\hat{x} + \hat{y}$ direction. The shadow region in the inset of Figure 5 is the irreducible Brillouin zone. The dotted envelope in Figure 5 corresponds to the plot for $\beta = k_0$, the boundary between bounded (slow wave) modes and leaky wave (fast wave) modes. In between X and M points, the bounded waves satisfy the Bragg condition in the \hat{x} direction, and there exist many improper complex modes.

IV. Acknowledgment

This work was supported in part by a contract from Phraxos R&D Inc.

V. References

- [1]. E. Yablonovitch, "Inhibited spontaneous emission in solid-state physics and electronics," *Physical Review Letters*, vol. 58, no. 20, pp. 2059-2062, May 1987.
- [2]. S.T. Peng, T. Tamir, H. Bertoni, "Theory of periodic dielectric waveguides," *IEEE Trans. on Microwave Theory and techniques*, vol. 23, no. 1, pp. 123-133, January 1975.
- [3]. E.W. Lucas, T.P. Fontana, "A 3-D hybrid finite element/boundary element method for the unified radiation and scattering analysis of general infinite periodic arrays," *IEEE Trans. on Antennas and Propagation*, vol. 43, no.2 , pp. 145-153, January 1995.
- [4]. C.F. Yang, W.D. Burnside, and R.C. Rudduck, "A double periodic moment method solution for the analysis and design of an absorber covered wall," *IEEE Trans. on Antennas and Propagation*, vol. 41, no.5 , pp. 600-601, May 1995.
- [5]. W. Platte, "Spectral dependence of light-induced microwave reflection coefficient from optoelectronic waveguide gratings," *IEEE Trans. on Microwave Theory and techniques*, vol. 43, no. 1, pp. 106-111, January 1995.
- [6]. S.D. Gedney, J.F. Lee, and R. Mittra, "A combined FEM/MoM approach to analyze the plane wave diffraction by arbitrary gratings," *IEEE Trans. on Microwave Theory and techniques*, vol. 40, no. 2, pp. 363-370, February 1992.
- [7]. S.I. Pereverzev and P.Y. Ufimtsev, "Permittivity and Permeability of a fiber grating," *Electromagnetics*, no 14, pp. 137-151, 1994.
- [8]. W.P. Pinello, R. Lee, and A.C. Cangellaris, "Finite element modeling of electromagnetic wave interactions with periodic dielectric structures," *IEEE Trans. on Microwave Theory and techniques*, vol. 42, no. 12, pp. 2294-2301, December 1994.

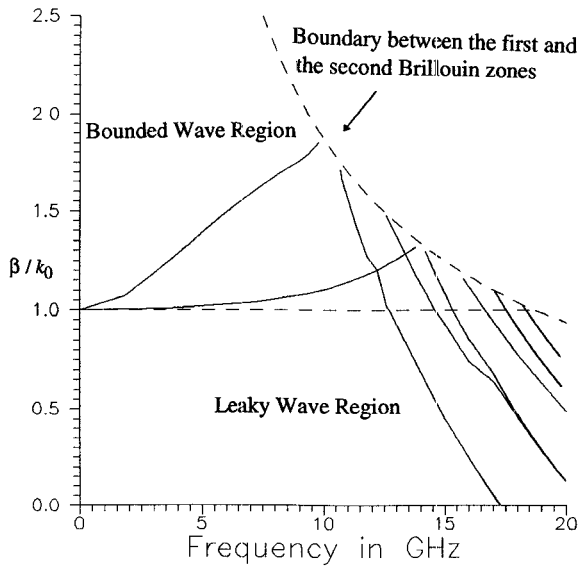


Figure 3. Dispersion diagram for modes in a dielectric slab with 2D material gratings. Propagation in the \hat{x} direction. $a = b = 8$ mm, $h = 4$ mm, $W = L = 6.4$ mm, $T = 3.2$ mm, $\Delta = 0.8$ mm, $\epsilon_1 = 4.0$, and $\epsilon_2 = 9.0$

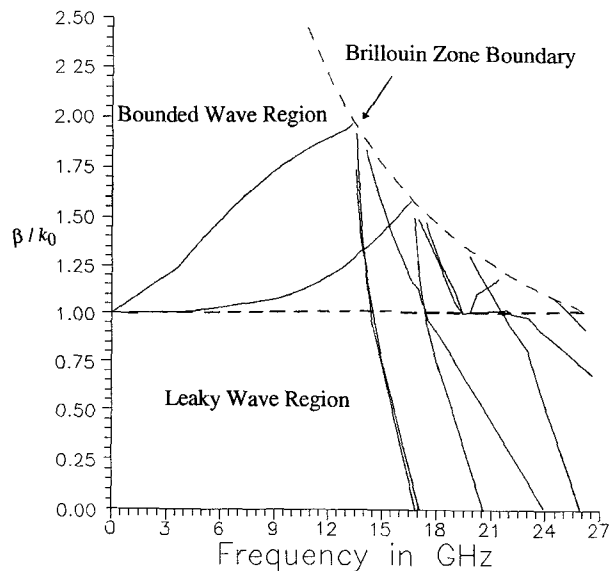


Figure 4. Dispersion diagram for modes in a dielectric slab with 2D material gratings. Propagation in the $\hat{x} + \hat{y}$ direction. Parameters are the same as those in Figure 3.

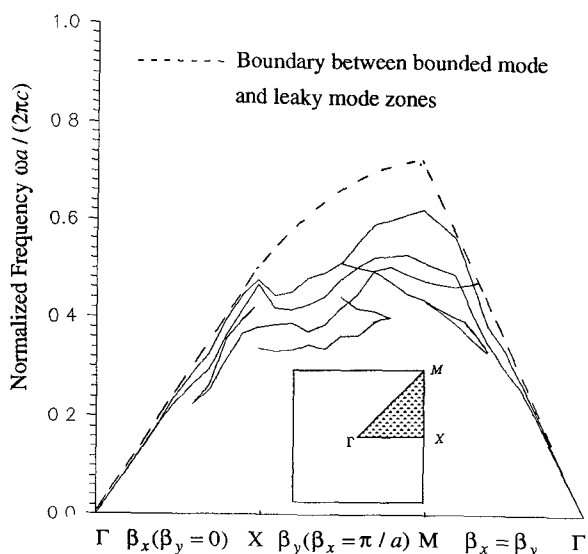


Figure 5. Photonic band structures for the bounded modes of a dielectric slab with 2D material gratings. $a = b = 8$ mm, $h = 4$ mm, $W = L = 6$ mm, $T = 4$ mm, $\Delta = 0$, $\epsilon_1 = 4$, and $\epsilon_2 = 1$. (Γ, X, M are symmetric points in Brillouin zone shown in the inset).